On the thermal broadening of zero-phonon impurity lines in absorption and fluorescence spectra

Cite as: J. Chem. Phys. **81**, 1604 (1984); https://doi.org/10.1063/1.447874
Submitted: 09 March 1984 . Accepted: 24 April 1984 . Published Online: 31 August 1998

D. Hsu, and J. L. Skinner

On the thermal broadening of zero-phonon impurity lines in absorption and fluorescence spectra

D. Hsu and J. L. Skinner
Department of Chemistry, Columbia University, New York, New York 10027

(Received 9 March 1984; accepted 24 April 1984)

We examine the problem of the absorption zero-phonon line shape for dilute impurities in crystals. We consider the usual two level electronic model, where both the ground and excited state Born–Oppenheimer surfaces are harmonic in the phonon coordinates. The difference between the two surfaces (the electron–phonon interaction) has terms which are both linear and quadratic in the phonon coordinates. In contrast to the usual perturbative theories, we calculate the zero–phonon line broadening and shift *to all orders* in the electron–phonon interaction. We find that only the quadratic term is responsible for line broadening, and that at $T = 0$ K this contribution vanishes. Our results are presented as integrals, which can be performed analytically or numerically, involving the weighted phonon density of states. We also show that within the model, the zero-phonon lines in the absorption and fluorescence spectra coincide exactly for all temperatures. Our results resolve the theoretical controversy produced by the two previous attempts to solve the line shape problem for strongly coupled electron–phonon systems. The work by Osad'ko is shown to be correct.

I. INTRODUCTION

Optical spectroscopy of isolated impurities in crystals provides information about the coupling of impurity electronic and lattice vibrational degrees of freedom—the electron–phonon coupling.[1-7] Substantial effort has been directed towards understanding the nature of the electron–phonon coupling, not only because of its intrinsic interest, but also because this coupling is often responsible for energy transfer between impurities in concentrated systems,[8] or for exciton scattering in pure systems.[9] For isolated impurities, the electron–phonon coupling produces characteristic phonon sidebands in optical absorption and fluorescence spectra. The sidebands result from an electronic transition with the accompanying absorption or emission of one or more phonons. In addition, one often observes a sharp zero-phonon line, resulting from a purely electronic transition. This zero-phonon line is, however, broadened and shifted by the electron–phonon coupling. It is the temperature dependence of this broadening and shift that concerns us in this paper.

At high temperatures, one can measure the broadening and shift directly from the absorption or fluorescence spectrum. However, at low temperatures, when the homogeneous linewidth becomes very small, the absorption or fluorescence linewidths are dominated by inhomogeneities, and the homogeneous linewidth cannot be observed. In this case, photon echo,[1-4] hole burning,[10] and fluorescence line narrowing[11] techniques have proven to be useful in extracting the homogeneous linewidth.

Theories of the zero-phonon line (ZPL) width and shift in absorption and fluorescence spectra have primarily been confined to *weak* electron–phonon coupling.[12-15] The usual model includes both linear and quadratic coupling. The ZPL width and shift are then calculated to lowest order in the coupling strength. For acoustic phonons in the Debye approximation it is found that the low temperature linewidth is proportional to T^7. This behavior has been observed experimentally.[12,16]

However, from the observed magnitude of the phonon sideband in many systems, it is not clear that the weak coupling assumption is justified. Perhaps this fact motivated two researchers to extend the above results into the strong coupling regime, i.e., to perform a nonperturbative calculation of the width and shift. Both Abram[17] and Osad'ko[18] considered linear and quadratic coupling to harmonic phonons, although the models are slightly different in that Abram made the rotating wave approximation in the quadratic term. Both workers found that linear coupling does not produce a temperature dependent broadening or shift of the line. But the results they obtained for the quadratic coupling are not in agreement. In particular, Abram[17] found that the shift is an odd function of the quadratic coupling strength, while the broadening is an even function. Osad'ko[18] obtained no such simplifications. Since this discrepancy cannot be traced back to the model differences, it is clear that one of the calculations is incorrect. Inasmuch as both works have been cited in the recent literature of ZPL broadening,[2,4,6,7] it seems important to resolve the discrepancy.

Most theories of the photon echo are also based on the weak coupling approach.[4] It is assumed that the system can be described by a two-level Bloch equation and the dephasing rate constant $1/T_2$ is calculated to lowest order in perturbation theory. One finds that this calculation is equivalent to the absorption linewidth calculation. It might be noted that at the very low temperatures at which these photon echo experiments are performed, dephasing by acoustic phonons seems to be unimportant. Instead, workers usually assume a sharply peaked density of states appropriate for a pseudolocal phonon. A calculation[2,7,19] based on this model leads to an Arrhenius temperature dependence of $1/T_2$, as observed experimentally.[1-4]

Recently, Skinner[20] showed that even for strong elec-

 0021-9606/84/161604-10$02.10

tron–phonon coupling, many properties of the system can be adequately described by a two-level Bloch equation as long as $1/T_2$ is calculated to all orders in perturbation theory. He also showed that $1/T_2$ is related to the homogeneous linewidth in the usual way: $\Delta\nu = 1/\pi T_2$. In addition, he provided formal nonperturbative expressions for $1/T_2$ in terms of the microscopic Hamiltonian.

The purpose of this paper is to calculate nonperturbatively the temperature dependent width and shift of the zero-phonon line using the expressions provided by Skinner[20] in order to resolve the discrepancy between Abram[17] and Osad'ko.[18] These authors express the dipole correlation function in a diagrammatic series and extract the linewidth and shift from the long time limit. Our method differs in that we take the long time limit in the beginning of the calculation, allowing us to express the width and shift *directly* as a diagrammatic series. This facilitates the summing of diagrams and avoids the need to solve an integral equation.[18,21] Our results are in complete agreement with Osad'ko[18] but not with Abram.[17] We also agree with Osad'ko[18] in finding that within our model, for any system the ZPL in absorption and the ZPL in fluorescence coincide exactly in both position and width. In a future paper[22] we will evaluate our strong coupling expressions for different phonon models and compare our results with experiment.

II. ZERO-PHONON LINEWIDTH AND SHIFT

For an isolated impurity in a crystal, we consider a model with only two electronic states. Within the Born–Oppenheimer approximation, the Hamiltonian is

$$H = |0\rangle\langle 0|H_0 + |1\rangle\langle 1|H_1, \tag{1}$$

where $|0\rangle$ and $|1\rangle$ are the ground and excited impurity electronic states, and H_0 and H_1 are the ground and excited state phonon Hamiltonians:

$$H_0 = T + V_0, \tag{2}$$

$$H_1 = T + V_1. \tag{3}$$

Here T is the nuclear kinetic energy operator and V_0 and V_1 are the Born–Oppenheimer ground and excited state potential surfaces. Within the harmonic approximation, the ground state Hamiltonian is

$$H_0 = \sum_k \hbar\omega_k (b_k^+ b_k + 1/2), \tag{4}$$

where b_k^+ and b_k are the creation and annihilation operators for the k th normal mode, and ω_k are the normal mode frequencies. The difference between the potential energies can be expanded in a Taylor series in the *ground* state normal mode coordinates. Keeping up to quadratic terms, we obtain

$$V_1 - V_0 = \hbar\omega_0 + \sum_k g_k (b_k^+ + b_k) + \frac{1}{2}\sum_{kq} g_{kq}(b_k^+ + b_k)(b_q^+ + b_q), \tag{5}$$

where ω_0 is a constant and g_k and g_{kq} are the linear and quadratic expansion coefficients. In what follows, we will actually adopt a less general form for the potential difference. We assume that it can be expanded in a single function ϕ which is linear in the normal mode coordinates

$$V_1 - V_0 = \hbar\omega_0 + a\phi + \frac{W}{2}\phi^2, \tag{6}$$

$$\phi = \sum_k h_k (b_k^+ + b_k), \tag{7}$$

where a and W are constants. We choose W to be dimensionless; thus h_k and a have units of the square root of energy. This functional form is correct if local strain is responsible for the energy difference[15] or if the impurity couples strongly to a *single* host molecule.[18] In other situations, Eq. (6) may in fact be a severe approximation. It should be realized, however, that it is precisely this approximation (in some guise or another) that has been made in previous theories[12–15,17,18] of ZPL thermal broadening and shift.

The optical absorption line shape is given by[23]

$$I(\omega) \propto \int_{-\infty}^{\infty} dt\, e^{i\omega t} e^{-|t|/2T_1} \langle\langle \mu(t)\mu(0)\rangle\rangle, \tag{8}$$

where

$$\mu(t) = e^{iHt/\hbar}\mu e^{-iHt/\hbar}, \tag{9}$$

and

$$\langle\langle \cdots \rangle\rangle = \mathrm{Tr}[e^{-\beta H} \cdots]/\mathrm{Tr}[e^{-\beta H}]. \tag{10}$$

(The double bracket indicates that the trace is over both electron and phonon degrees of freedom.) T_1 is the excited state lifetime and μ is the transition dipole operator, which in the Condon approximation is

$$\mu = \mu_0(|0\rangle\langle 1| + |1\rangle\langle 0|), \tag{11}$$

where μ_0 is a constant. Performing the electronic trace, we obtain

$$I(\omega) \propto \int_{-\infty}^{\infty} dt\, e^{i(\omega-\omega_0)t} e^{-|t|/2T_1} \langle F(t)\rangle, \tag{12}$$

where

$$F(t) = \exp(iH_0 t/\hbar)\exp[-i(\Delta + H_0)t/\hbar], \tag{13}$$

$$\Delta = A + B, \tag{14}$$

$$A = a\phi, \tag{15}$$

$$B = \frac{W}{2}\phi^2, \tag{16}$$

and

$$\langle \cdots \rangle = \mathrm{Tr}_p[e^{-\beta H_0} \cdots]/\mathrm{Tr}_p[e^{-\beta H_0}]. \tag{17}$$

Here the brackets indicate a thermal phonon average with the ground state phonon Hamiltonian. $F(t)$ can also be written as

$$F(t) = \exp_T\left[\frac{-i}{\hbar}\int_0^t d\tau\, \Delta(\tau)\right], \tag{18}$$

where

$$\Delta(\tau) = e^{iH_0\tau/\hbar}\Delta e^{-iH_0\tau/\hbar}, \tag{19}$$

and T is the chronological operator that orders the $\Delta(\tau)$'s in order of increasing time from right to left for $t > 0$ and from left to right for $t < 0$.

It is convenient to perform a cumulant expansion[24] of $\langle F(t)\rangle$:

$$\langle F(t)\rangle = \exp\left[\sum_{m=1}^{\infty} K_m(t)\right], \tag{20}$$

$$K_m(t) = (-i/\hbar)^m (m!)^{-1} \int_0^t d\tau_1 \int_0^t d\tau_2 \cdots \int_0^t d\tau_m \times \langle T\Delta(\tau_1)\Delta(\tau_2)\cdots\Delta(\tau_m)\rangle_c. \tag{21}$$

$\langle\cdots\rangle_c$ denotes a cumulant average. Since it is the long time behavior of $\langle F(t)\rangle$ that determines the position and shape of the ZPL,[5] we focus on that here. Skinner[20] showed that for $t \gg \tau_c$, where τ_c is the phonon correlation time [the time in which $\langle \Delta(\tau)\Delta(0)\rangle$ decays], then

$$K_m(t) \propto tK_m, \quad t \gg \tau_c, \tag{22}$$

$$K_m = (-i/\hbar)^m \int_0^\infty d\tau_1 \int_0^\infty d\tau_2 \cdots \int_0^\infty d\tau_{m-1} \times \langle T\Delta(\tau_1+\tau_2+\cdots\tau_{m-1})\cdots\Delta(\tau_1)\Delta(0)\rangle_c. \tag{23}$$

(In Ref. 20 the time ordering operator does not appear in the equation. Here it will be convenient to use the above form. The two expressions are of course equivalent since the Δ's are already time ordered.) Defining

$$K = \sum_{m=1}^{\infty} K_m, \tag{24}$$

$$\gamma = -\mathrm{Re}\{K\}, \tag{25}$$

and

$$\delta = -\mathrm{Im}\{K\}, \tag{26}$$

then

$$\langle F(t)\rangle \propto \exp[-(\gamma + i\delta)t]. \tag{27}$$

Considering negative times as well, for $|t| \gg \tau_c$ one finds that

$$\langle F(t)\rangle \propto e^{-\gamma|t|} e^{-i\delta t}. \tag{28}$$

Substituting this into Eq. (12), we find that the ZPL is Lorentzian;

$$I_{\mathrm{ZPL}}(\omega) \propto [(\omega - (\omega_0 + \delta))^2 + \Gamma^2]^{-1}, \tag{29}$$

$$\Gamma = \gamma + 1/2T_1, \tag{30}$$

with position $(\omega_0 + \delta)$ and width $(\gamma + 1/2T_1)$. Thus the line shift δ and the pure dephasing contribution to the linewidth γ are the imaginary and real parts of an infinite sum of cumulants.

In what follows, we will express each term K_m of the cumulant sum as a sum of diagrams. A judicious resummation of the resulting infinite series gives a closed form analytic expression.

The first few terms of the series are easily written down. with Eqs. (14)–(16) and (23), we find that

$$K_1 = (-i/\hbar)(W/2)C(0), \tag{31}$$

where the time-ordered correlation function (Green's function) $C(t)$ is defined to be

$$C(t) = \langle T\phi(t)\phi(0)\rangle. \tag{32}$$

Using Eq. (7) this becomes

$$C(t) = \sum_k h_k^2 [(n_k+1)e^{-i\omega_k|t|} + n_k e^{i\omega_k|t|}], \tag{33}$$

where

$$n_k = n(\omega_k) = [\exp(\beta\hbar\omega_k) - 1]^{-1}. \tag{34}$$

For K_2, explicitly writing the cumulant average we have

$$K_2 = (-i/\hbar)^2 \int_0^\infty dt_1 \{\langle T\Delta(t_1)\Delta(0)\rangle - \langle\Delta(t_1)\rangle\langle\Delta(0)\rangle\} \tag{35}$$

$$= (-i/\hbar)^2 \int_0^\infty dt_1 \{\langle TA(t_1)A(0)\rangle + \langle TB(t_1)B(0)\rangle - \langle B\rangle^2\rangle\}. \tag{36}$$

Using Eq. (16), we write

$$\langle TB(t)B(0)\rangle = (W/2)^2\langle T\phi(t)\phi(t)\phi(0)\phi(0)\rangle. \tag{37}$$

With the finite-temperature version of Wick's theorem,[25] we can express the right-hand side as the sum of all possible contractions, leaving

$$\langle TB(t)B(0)\rangle = (W/2)^2\{2C(t)^2 + C(0)^2\}. \tag{38}$$

Thus the second cumulant is

$$K_2 = (-i/\hbar)^2 \int_0^\infty dt_1 \{a^2 C(t_1) + (W^2/2)C(t_1)^2\}. \tag{39}$$

Similarly for K_3 we have

$$K_3 = (-i/\hbar)^3 \int_0^\infty dt_1 \int_0^\infty dt_2 \{\langle A(t_1+t_2)A(t_1)B(0)\rangle_c + \langle A(t_1+t_2)B(t_1)A(0)\rangle_c + \langle B(t_1+t_2)A(t_1)A(0)\rangle_c + \langle B(t_1+t_2)B(t_1)B(0)\rangle_c\}. \tag{40}$$

Using Wick's theorem and performing the cumulant average, one obtains

$$K_3 = (-i/\hbar)^3 \int_0^\infty dt_1 \int_0^\infty dt_2 \{a^2\, WC(t_1+t_2)C(t_1) + a^2\, WC(t_1)C(t_2) + a^2\, WC(t_1+t_2)C(t_2) + W^3\, C(t_1)C(t_2)C(t_1+t_2)\}. \tag{41}$$

These three terms are conveniently represented by diagrams as in Fig. 1. The rules for evaluating these diagrams are as follows:

(i) a line joining two points (a point is a dot or circle) represents a factor $C(t)$;

(ii) with each point is associated a time argument; 0 with the left most point, t_1 with the next point to the right, $t_1 + t_2$ with the next point to the right, etc.;

(iii) the time argument of a factor $C(t)$ represented by a

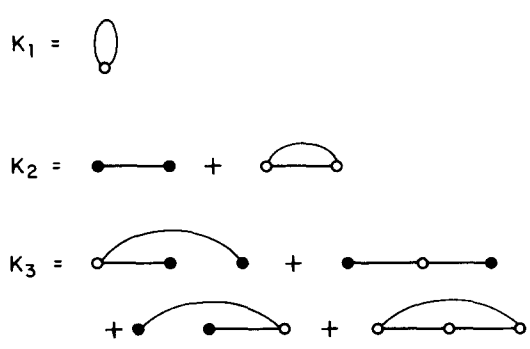

FIG. 1. Diagrammatic representation of the first three terms in the cumulant expansion.

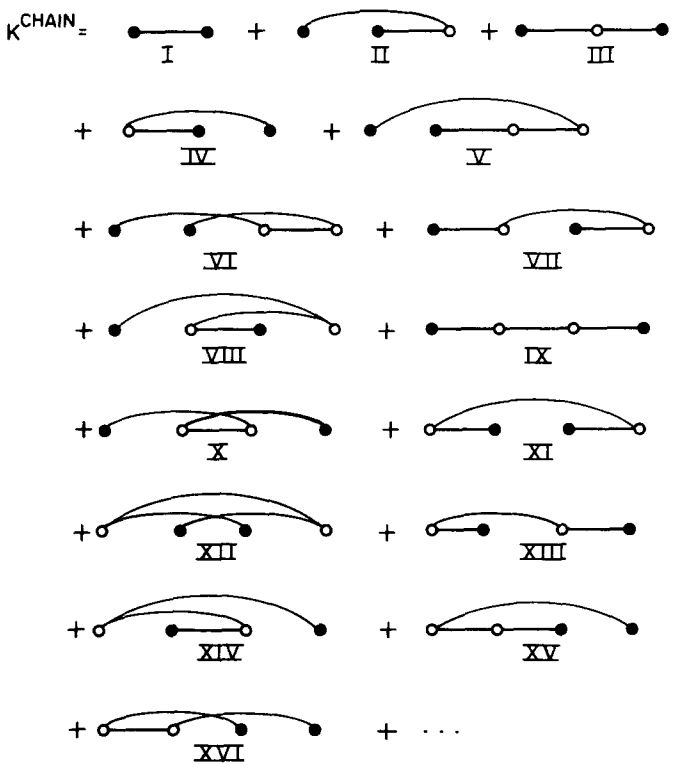

FIG. 2. The chain diagrams that contribute to the cumulant sum.

line joining two points is the time associated with the right point minus the time associated with the left point;

(iv) for a diagram with m points, there are $m-1$ time integrals of the form

$$\int_0^\infty dt_1 \int_0^\infty dt_2 \cdots \int_0^\infty dt_{m-1};$$

(v) with each dot is associated a factor $-ia/\hbar$;

(vi) with each circle is associated a factor $-iW/\hbar$;

(vii) if the two lines from each circle do not go to two different points, there is a factor of 1/2.

It is easy to see how to generalize the diagrammatic method to the higher cumulants. It is important to note that because of the cumulant average, only *connected* diagrams remain. All the diagrams can be classified into two types—those with only circles, which we call loop diagrams, and those with exactly two dots, which we call chain diagrams. The rules for constructing the mth order loop diagrams are as follows:

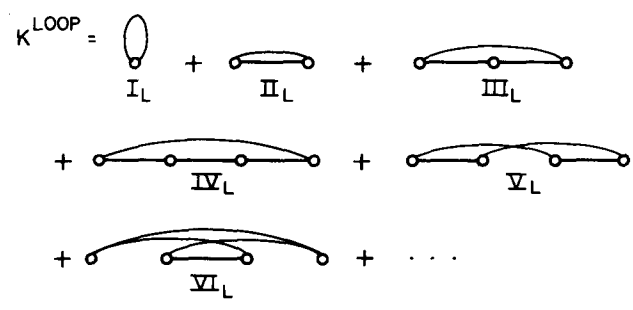

FIG. 3. The loop diagrams that contribute to the cumulant sum.

(i) connect m circles, arranged horizontally, with lines in all possible ways such that each circle has two lines and the diagram remains connected.

The rules for constructing the mth order chain diagrams are as follows:

(i) arrange two dots and $m-2$ circles horizontally in all possible ways;

(ii) for each arrangement connect the dots and circles with lines in all possible ways such that each dot has exactly one line and each circle has exactly two lines and the diagram remains connected.

Writing

$$K = K^{\text{loop}} + K^{\text{chain}}, \tag{42}$$

we obtain the diagrammatic representation shown in Figs. 2 and 3.

A. Chain diagrams

First we will consider the chain diagrams shown in Fig. 2. For example,

$$I = (-i/\hbar)^2 \int_0^\infty dt_1\, a^2 C(t_1). \tag{43}$$

Defining the Fourier transform

$$\hat{C}(\omega) = \int_{-\infty}^{\infty} dt\, e^{i\omega t} C(t) \tag{44}$$

and using the fact that $C(t)$ is even in time, Eq. (43) becomes

$$I = (-i/\hbar)^2 (a^2/2)\hat{C}(0). \tag{45}$$

For future use, we note that using Eq. (33), $\hat{C}(\omega)$ can be computed explicitly, with the result

$$\hat{C}(\omega) = (2n(\omega)+1)\hbar\Gamma(\omega) + (2n(-\omega)+1) \times \hbar\Gamma(-\omega) + i\hbar\Omega(\omega), \tag{46}$$

where

$$\Gamma(\omega) = \left(\frac{\pi}{\hbar}\right) \sum_k h_k^2\, \delta(\omega - \omega_k), \tag{47}$$

and

$$\Omega(\omega) = \left(\frac{1}{\hbar}\right) \sum_k h_k^2 \left\{ P\left(\frac{1}{\omega - \omega_k}\right) - \left(\frac{1}{\omega + \omega_k}\right)\right\}. \tag{48}$$

This can also be written as

$$\Omega(\omega) = \int_0^\infty \frac{d\omega'}{\pi} \Gamma(\omega') 2\omega' P\left(\frac{1}{\omega^2 - \omega'^2}\right). \tag{49}$$

In the above, $\Gamma(\omega)$ is the dimensionless weighted phonon density of states. Since all $\omega_k > 0$, it follows that $\Gamma(-\omega) = 0$ for $\omega \geqslant 0$. Thus

$$I = \left(\frac{-i}{\hbar}\right)\left(\frac{a^2}{2}\right)\Omega(0). \tag{50}$$

Similarly

$$\text{III} = (-i/\hbar)^3 \int_0^\infty dt_1 \int_0^\infty dt_2\, a^2\, WC(t_1)C(t_2) \tag{51}$$

$$= \left(\frac{-i}{\hbar}\right)^3 a^2\, W \left(\frac{\Omega(0)}{2}\right)^2. \tag{52}$$

The diagram

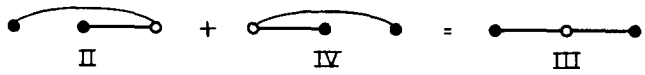

FIG. 4. The diagrammatic sum of two third order chain diagrams.

$$\text{II} = (-i/h)^3 \int_0^\infty dt_1 \int_0^\infty dt_2\, a^2\, WC(t_1+t_2)C(t_2), \quad (53)$$

is not as straightforward to evaluate. However, if we make the change of variables $\tau_1 = t_1 + t_2$, $\tau_2 = t_2$, we have

$$\text{II} = (-i/\hbar)^3 \int_0^\infty d\tau_1 \int_0^{\tau_1} d\tau_2\, a^2\, WC(\tau_1)(C\tau_2). \quad (54)$$

Similarly, for IV,

$$\text{IV} = (-i/\hbar)^3 \int_0^\infty dt_1 \int_0^\infty dt_2\, a^2\, WC(t_1)C(t_1+t_2), \quad (55)$$

if we make the change of variables $\tau_1 = t_1$, $\tau_2 = t_1 + t_2$, we have

$$\text{IV} = (-i/\hbar)^3 \int_0^\infty d\tau_1 \int_{\tau_1}^\infty d\tau_2\, a^2\, WC(\tau_1)C(\tau_2). \quad (56)$$

Thus it is clear that these two diagrams can be added together to obtain the diagram sum shown in Fig. 4.

For the higher order chains it is difficult to evaluate the diagrams separately. However, they can be added together appropriately to obtain simple results. To this end, within each order of chain diagrams, we introduce certain diagram classes. To obtain the class of a given mth order diagram, one starts with the left most dot and numbers the lines sequentially from 1 to $m-1$. At each circle, the lines either come from different sides or the same side. Let us associate a $+$ sign with the former, and a $-$ sign with the latter. The class of a diagram is given by the ordered sequence of pluses and minuses corresponding to the senses of the circles in going from line 1 to line $m-1$. An example of a numbered sixth order diagram and its class is shown in Fig. 5.

The only mth order diagram of the class $(+\ +\cdots+)$ is shown in Fig. 6. It is straightforward to evaluate:

$$\text{XVII} = \left(\frac{-i}{\hbar}\right) a^2\, W^{m-2} \left(\frac{\Omega(0)}{2}\right)^{m-1}. \quad (57)$$

One finds that for any diagram class of any diagram order, the sum of the diagrams in the class is equal to the single diagram of the $(+\ +\cdots+)$ class for that order. For example, the fourth order diagrams of the $(-\ +)$ class are shown in Fig. 7:

$$\text{V} = (-i/\hbar)^4 a^2 W^2 \int_0^\infty dt_1 \int_0^\infty dt_2 \int_0^\infty dt_3 C(t_2)C(t_3) \times C(t_1+t_2+t_3), \quad (58)$$

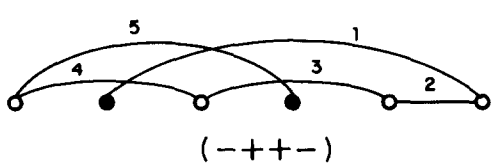

FIG. 5. A numbered sixth order chain diagram of the class $(-\ +\ +\ -)$.

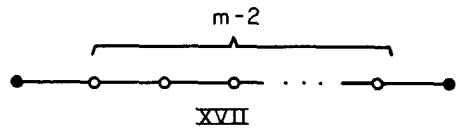

FIG. 6. The only mth order chain diagram of the class $(+\ +\cdots+)$.

$$\text{XIII} = (-i/\hbar)^4 a^2 W^2 \int_0^\infty dt_1 \int_0^\infty dt_2 \int_0^\infty dt_3 C(t_1) \times C(t_1+t_2)C(t_3), \quad (59)$$

$$\text{XVI} = (-i/\hbar)^4 a^2 W^2 \int_0^\infty dt_1 \int_0^\infty dt_2 \int_0^\infty dt_3 C(t_1+t_2) \times C(t_1)C(t_2+t_3). \quad (60)$$

The numbering of the lines (see Fig. 7) now indicates the advantageous change of variables of each diagram. For example, in V we let $\tau_1 = t_1 + t_2 + t_3$, $\tau_2 = t_3$, and $\tau_3 = t_2$, leaving

$$\text{V} = (-i/\hbar)^4 a^2 W^2 \int_0^\infty d\tau_1 \int_0^{\tau_1} d\tau_2 \int_0^{\tau_1-\tau_2} d\tau_3\, C(\tau_1) \times C(\tau_2)C(\tau_3). \quad (61)$$

Similarly, for the other two diagrams, we obtain

$$\text{XIII} = (-i/\hbar)^4 a^2 W^2 \int_0^\infty d\tau_1 \int_{\tau_1}^\infty d\tau_2 \times \int_0^\infty d\tau_3 C(\tau_1)C(\tau_2)C(\tau_3), \quad (62)$$

$$\text{XVI} = (-i/\hbar)^4 a^2 W^2 \int_0^\infty d\tau_1 \int_0^{\tau_1} d\tau_2 \times \int_{\tau_1-\tau_2}^\infty C(\tau_1)C(\tau_2)C(\tau_3). \quad (63)$$

The integration limits are such that these three expressions can be summed to give

$$\text{V} + \text{XIII} + \text{XVI} = (-i/\hbar)^4 a^2 W^2 \int_0^\infty d\tau_1 \int_0^\infty d\tau_2 \times \int_0^\infty d\tau_3 C(\tau_1)C(\tau_2)C(\tau_3). \quad (64)$$

This is shown diagrammatically in Fig. 8.

Since there are $m-2$ circles in an mth order chain diagram, there are $2^{(m-2)}$ diagram classes. Therefore since the sum of all diagrams in a class is equal to the $(+\ +\cdots+)$ diagram, the chain sum is shown in Fig. 9. Using Eq. (57) this sum becomes

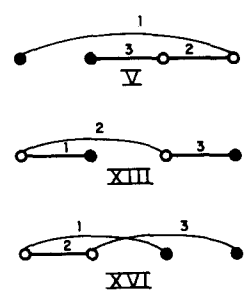

FIG. 7. The three fourth order chain diagrams of the class $(-\ +)$.

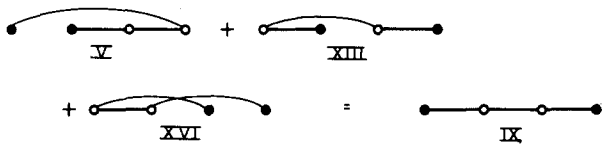

FIG. 8. The diagrammatic sum of the fourth order chain diagrams of the class (− +).

$$K^{\text{chain}} = \left(\frac{-i}{\hbar}\right)\frac{a^2\Omega(0)}{2}(1 - W\Omega(0))^{-1}. \tag{65}$$

B. Loop diagrams

Next we consider the loop diagrams of Fig. 3. I_L has been discussed previously and is given by Eq. (31). Writing $C(t)$ in terms of its Fourier transform

$$C(t) = \frac{1}{2\pi}\int_{-\infty}^{\infty} d\omega\, e^{-i\omega t}\hat{C}(\omega), \tag{66}$$

and using the fact that $C(t)$ is even, we obtain

$$\mathrm{I}_L = \frac{-iW}{\hbar}\int_0^{\infty}\frac{d\omega}{2\pi}\hat{C}(\omega). \tag{67}$$

For the second order loop, we have [do not forget rule (vii) for the evaluation of this diagram]

$$\mathrm{II}_L = \left(\frac{-iW}{\hbar}\right)^2\frac{1}{4}\int_{-\infty}^{\infty} dt\, C(t)^2. \tag{68}$$

Substituting in Eq. (66) for each $C(t)$ we find

$$\mathrm{II}_L = \left(\frac{-iW}{\hbar}\right)^2\frac{1}{2}\int_0^{\infty}\frac{d\omega}{2\pi}\hat{C}(\omega)^2. \tag{69}$$

Now let us consider the higher loop diagrams. We will again find it useful to assign each diagram to a diagram class. To do so, however, the diagrams must be numbered. For the chains, we numbered the lines sequentially starting from the leftmost dot. For the loops, there are no dots and hence no unambiguous starting points. Nonetheless, the appropriate procedure is as follows: For each diagram, pick an arbitrary line and imagine that the circles at the ends of the line are dots; then number the diagram as if it were a chain diagram. For an mth order diagram, there are m different possible numberings. It is convenient to include them all and divide the result by m. For each numbered diagram, the diagram class is found in the same manner as for chain diagrams. (The circles connected by line m are considered dots for the purpose of assigning diagram classes.)

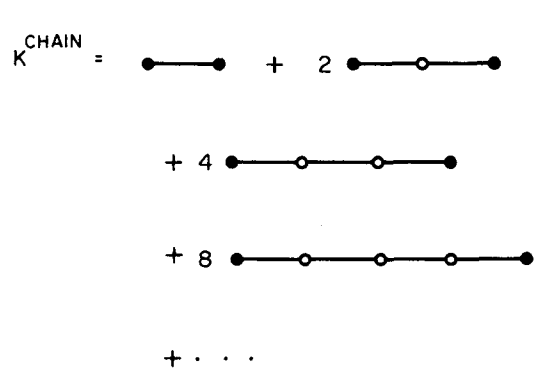

FIG. 9. The diagrammatic sum of all the chain diagrams.

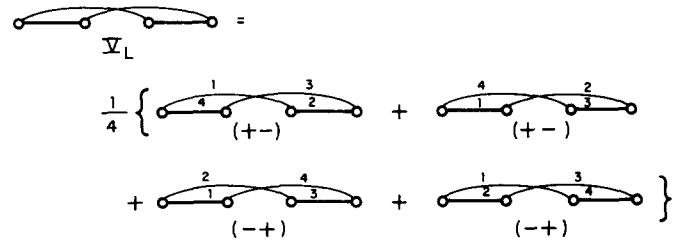

FIG. 10. The decomposition of a fourth order loop diagram into numbered diagrams. The class of each numbered diagram is also shown.

An example of the above procedure is shown in Fig. 10 for the fourth order loop diagram V_L. When this procedure is followed for all three fourth order loop diagrams, 12 numbered diagrams in four classes are generated. For example, the three fourth order numbered diagrams of the (− +) class are shown in Fig. 11. The expressions are

$$\mathrm{VII}_L = \mathrm{VIII}_L = \left(\frac{-iW}{\hbar}\right)^4\int_0^{\infty} dt_1\int_0^{\infty} dt_2\int_0^{\infty} dt_3\, C(t_1) \times C(t_1+t_2)C(t_2+t_3)C(t_3), \tag{70}$$

$$\mathrm{IX}_L = \left(\frac{-iW}{\hbar}\right)^4\int_0^{\infty} dt_1\int_0^{\infty} dt_2\int_0^{\infty} dt_3\, C(t_1)C(t_2)C(t_3) \times C(t_1+t_2+t_3). \tag{71}$$

As before, the appropriate variable changes are determined by the numbering scheme. Thus for VII_L, we let $\tau_1 = t_1$, $\tau_2 = t_1 + t_2$, and $\tau_3 = t_3$, and find

$$\mathrm{VII}_L = \left(\frac{-iW}{\hbar}\right)^4\int_0^{\infty} d\tau_1\int_{\tau_1}^{\infty} d\tau_2\int_0^{\infty} d\tau_3 \times C(\tau_1)C(\tau_2)C(\tau_3)C(\tau_2-\tau_1+\tau_3). \tag{72}$$

Similarly for VIII_L and IX_L we obtain

$$\mathrm{VIII}_L = \left(\frac{-iW}{\hbar}\right)^4\int_0^{\infty} d\tau_1\int_0^{\tau_1} d\tau_2\int_{\tau_1-\tau_2}^{\infty} d\tau_3 C(\tau_1)C(\tau_2) \times C(\tau_3)C(\tau_2-\tau_1+\tau_3), \tag{73}$$

$$\mathrm{IX}_L = \left(\frac{-iW}{\hbar}\right)^4\int_0^{\infty} d\tau_1\int_0^{\tau_1} d\tau_2\int_0^{\tau_1-\tau_2} d\tau_3 C(\tau_1)C(\tau_2) \times C(\tau_3)C(\tau_1-\tau_2-\tau_3). \tag{74}$$

Because $C(t)$ is even, these three diagrams can be summed to obtain

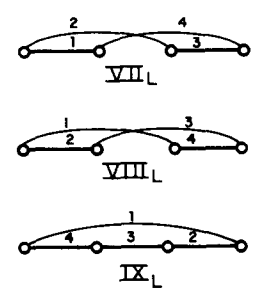

FIG. 11. The three fourth order numbered loop diagrams of the class (− +).

$$\mathrm{VII}_L + \mathrm{VIII}_L + \mathrm{IX}_L = \left(\frac{-iW}{\hbar}\right)^4 \int_0^\infty d\tau_1 \int_0^\infty d\tau_2 \int_0^\infty d\tau_3 C(\tau_1)C(\tau_2) \times C(\tau_3)C(\tau_1-\tau_2-\tau_3). \tag{75}$$

If similar manipulations are performed on the other diagram classes [(+ +), (+ −), and (− −)], one finds that the sum of all the fourth order loop diagrams K_4^{loop} is given by

$$K_4^{\mathrm{loop}} = \left(\frac{-iW}{\hbar}\right)^4 \frac{1}{4} \int_0^\infty d\tau_1 \times \int_0^\infty d\tau_2 \int_0^\infty d\tau_3 C(\tau_1)C(\tau_2)C(\tau_3)\{C(\tau_1+\tau_2+\tau_3) + C(\tau_1+\tau_2-\tau_3) + C(\tau_1-\tau_2-\tau_3) + C(\tau_1-\tau_2+\tau_3)\}. \tag{76}$$

Using the fact that $C(t)$ is even, we can rewrite this as

$$K_4^{\mathrm{loop}} = \left(\frac{-iW}{\hbar}\right)^4 \frac{1}{8} \int_{-\infty}^\infty d\tau_1 \int_{-\infty}^\infty d\tau_2 \int_{-\infty}^\infty d\tau_3 \times C(\tau_1)C(\tau_2)C(\tau_3)C(\tau_1+\tau_2+\tau_3). \tag{77}$$

Using Eq. (66) we obtain

$$K_4^{\mathrm{loop}} = \left(\frac{-iW}{\hbar}\right)^4 \frac{1}{4} \int_0^\infty \frac{d\omega}{2\pi} \hat{C}(\omega)^4. \tag{78}$$

For higher order loops, these results generalize immediately. For the mth order loop diagrams there are $2^{(m-2)}$ diagram classes. First the diagrams in each class are summed and then the classes are summed to obtain

$$K_m^{\mathrm{loop}} = \left(\frac{-iW}{\hbar}\right)^m \frac{1}{m} \int_0^\infty \frac{d\omega}{2\pi} \hat{C}(\omega)^m. \tag{79}$$

Therefore we find finally that

$$K^{\mathrm{loop}} = \sum_{m=1}^\infty K_m^{\mathrm{loop}} = -\int_0^\infty \frac{d\omega}{2\pi} \ln\left[1 + iW\frac{\hat{C}(\omega)}{\hbar}\right]. \tag{80}$$

C. Results for the absorption ZPL

We have calculated the sum of all chain diagrams K^{chain} [Eq. (65)] and the sum of all loop diagrams K^{loop} [Eq. (80)]. From Eqs. (25), (26), and (42), this gives us the ZPL broadening and shift

$$\gamma + i\delta = -(K^{\mathrm{chain}} + K^{\mathrm{loop}}). \tag{81}$$

K^{chain} is purely imaginary and thus contributes only to the line shift. Moreover, K^{chain} is temperature independent. It is useful to write K^{loop} as a sum of zero temperature and temperature dependent components:

$$K^{\mathrm{loop}} = K_0^{\mathrm{loop}} + K_T^{\mathrm{loop}}. \tag{82}$$

Using Eq. (46) we obtain

$$K_0^{\mathrm{loop}} = -\int_0^\infty \frac{d\omega}{2\pi} \ln[1 - W\Omega(\omega) + iW\Gamma(\omega)], \tag{83}$$

$$K_T^{\mathrm{loop}} = -\int_0^\infty \frac{d\omega}{2\pi} \ln\left[1 + \frac{iW2n(\omega)\Gamma(\omega)}{1 - W\Omega(\omega) + iW\Gamma(\omega)}\right]. \tag{84}$$

Although it appears that K_0^{loop} has nonvanishing real and imaginary parts, in Appendix A we show that, in fact, $\mathrm{Re}\{K_0^{\mathrm{loop}}\} = 0$. Defining δ_0 and δ_T as the zero temperature and thermal ZPL line shifts, from the above arguments we see that

$$\delta = \delta_0 + \delta_T, \tag{85}$$

$$\delta_0 = iK^{\mathrm{chain}} - \mathrm{Im}\{K_0^{\mathrm{loop}}\}, \tag{86}$$

$$\gamma + i\delta_T = -K_T^{\mathrm{loop}}. \tag{87}$$

Taking the required real or imaginary parts gives

$$\delta_0 = \frac{a^2\Omega(0)}{2\hbar}(1 - W\Omega(0))^{-1} + \int_0^\infty \frac{d\omega}{2\pi} \arctan(W\Gamma(\omega)(1 - W\Omega(\omega))^{-1}), \tag{88}$$

$$\delta_T = \int_0^\infty \frac{d\omega}{2\pi} \times \arctan\left[\frac{2n(\omega)W\Gamma(\omega)(1 - W\Omega(\omega))}{(1 - W\Omega(\omega))^2 + (2n(\omega)+1)W^2\Gamma(\omega)^2}\right], \tag{89}$$

$$\gamma = \int_0^\infty \frac{d\omega}{4\pi} \ln\left[1 + \frac{4n(\omega)(n(\omega)+1)W^2\Gamma(\omega)^2}{(1 - W\Omega(\omega))^2 + W^2\Gamma(\omega)^2}\right]. \tag{90}$$

Equations (88)–(90) are the principle results of this paper. The broadening and shift depend only on the weighted phonon density of states $\Gamma(\omega)$ [Eq. (47)], the linear and quadratic coupling constants a and W, and the temperature. [$\Omega(\omega)$ is determined by $\Gamma(\omega)$ from Eq. (49).]

First of all, we note that when $T \to 0$ K, $n(\omega) \to 0$, and thus $\gamma \to 0$; there is no pure dephasing at $T = 0$ K. This is in accord with more general arguments.[26] Secondly, it is seen that when $W = 0$ (no quadratic coupling), $\gamma = 0$; linear coupling alone will not produce line broadening. The only effect of the linear coupling is a temperature independent line shift $\delta_0 = -(a^2/\hbar^2)\Sigma_k h_k^2/\omega_k$.

The principle results of this paper are in complete agreement with Osad'ko.[18] Expansion of the above results for small W gives agreement with the usual perturbative results.[12–15] Expansion to higher order in W shows that γ has contributions from quadratic and *all higher* powers of W, and that δ_T has contributions from linear and *all higher* powers of W. This observation is in contrast to Abram's results[17]—that γ contains only *even* powers of W and δ_T contains only *odd* powers of W. Although Abram used a slightly different model Hamiltonian (he made the rotating wave approximation in the quadratic term), the above discrepancy cannot be traced to this difference.[27] Thus we must conclude that Abram's result is incorrect.

D. Results for the fluorescence ZPL

The previous three sections have dealt with the ZPL in the absorption spectrum. It is also interesting to examine the ZPL in fluorescence spectra. It is especially important to make the connection between the two, since often both types of experiments are performed on the same system.

Our theoretical method is equally capable of calculat-

ing the ZPL properties in fluorescence. The essential difference between the two calculations involves the reversal of the roles played by the ground and excited state Born–Oppenheimer potential energies. Since both surfaces are harmonic, this reversal poses no particular problems. The details of the calculation are given in Appendix B. There we obtain the not altogether obvious result, also found by Osad'ko,[18] that (within our model) for a given impurity-phonon system, the width and shift of the ZPL's in fluorescence and absorption are identical at any temperature. Thus, although the phonon sideband structure of the two spectra are very different, the zero phonon lines should be superimposed. This coincidence of the two ZPL's is in fact observed experimentally.[7,18]

III. CONCLUDING REMARKS

We have considered the thermal broadening and shift of zero-phonon lines in the absorption and fluorescence spectroscopy of impurities in crystals. In our model, both the ground and excited electronic state Born–Oppenheimer surfaces are harmonic in phonon coordinates and their difference contains terms which are both linear and quadratic in these coordinates. We found that only the quadratic term produces a thermal broadening and shift of the zero-phonon line. In contrast to most theories of the shift and broadening, which are valid to only first or second order, respectively, in the quadratic coupling constant, our results are valid for arbitrarily strong coupling. Our results are in agreement with one[18] of the two previous attempts to solve this problem but not with the other.[17] We have also shown that for any system at any temperature, the zero-phonon lines in absorption and fluorescence should coincide exactly.

From a theoretical viewpoint, the solution given in this paper is novel in that the quantities of interest, the zero-phonon line broadening and shift, are *directly* expressed as a diagrammatic expansion. The resulting infinite series can be summed immediately to yield the final answer. In the more usual approach,[18,21] the *dipole correlation function* is represented diagrammatically. The resulting series is not summed directly, but leads to an integral equation. The long time limit of the solution to the integral equation then gives the final answer. For this particular problem the first approach seems more straightforward.

In this paper we have focused on the impurity line broadening and shift in absorption and fluorescence spectroscopy. At high temperatures, these low power (linear) methods are adequate for measuring linewidths. However, at low temperatures, since the homogeneous linewidths become very small and the systems are inhomogeneously broadened, nonlinear techniques such as hole burning, the photon echo, or fluorescence line narrowing must be used. Although it is not obvious, especially for systems *strongly* coupled to a bath such as our electron–phonon system, that nonlinear experiments and linear experiments are measuring the same quantities, Skinner[20] has shown that at least for the photon echo, this is indeed the case. If we assume that the same is true for hole burning and fluorescence line narrowing spectroscopies, then one has a variety of complementary techniques which can all be used to measure the homogeneous linewidth.

Thus we have a wealth of experimental data which should be analyzed with the strong coupling results. As a first step, one should evaluate these results for various phonon models. Some work in this direction has been performed by Osad'ko.[6,7,18] We[22] are also involved in this program. Preliminary work shows that for a Debye density of states, the linewidth is proportional to T^7 at low temperatures, in agreement with both weak coupling theory and experiment. Similarly, for a sharply peaked density of states, the linewidth is exponentially activated, also in agreement with weak coupling theory and experiment. Analysis of the experimental data, however, shows that most of the systems are *not* in the weak coupling regime. At higher temperature, the weak and strong coupling theories can differ dramatically. Analysis of experimental data with the strong coupling theory at these higher temperatures is in progress.[22]

ACKNOWLEDGMENTS

We thank the National Science Foundation, Grant No. DMR 83-06429, and the Donors of the Petroleum Research Fund, administered by the American Chemical Society, for support of this work.

APPENDIX A

Here we show that $\mathrm{Re}\{K_0^{\mathrm{loop}}\}=0$. By definition $K_0^{\mathrm{loop}}=K^{\mathrm{loop}}|^{T=0}$, where K^{loop} is the sum of all diagrams in Fig. 3. Each line in a diagram represents a factor $C(t)$. At $T=0$, $C(t)$ from Eq. (33) is replaced by

$$C_0(t)=\sum_k h_k^2 e^{-i\omega_k|t|}. \tag{A1}$$

The expression for any mth order loop diagram has $m-1$ time integrals from 0 to ∞. At $T=0$ K each one of these time integrals leads to a factor of i times a principal value. Since there is also an accompanying i^m for each mth order diagram, each diagram goes like i^{2m-1}. Thus every zero temperature loop diagram is purely imaginary and $\mathrm{Re}\{K_0^{\mathrm{loop}}\}=0$. As an example, consider the diagram V_L from Fig. 3 evaluated at $T=0$ K:

$$V_L|^{T=0}=\left(\frac{-iW}{\hbar}\right)^4\int_0^\infty dt_1\int_0^\infty dt_2\int_0^\infty dt_3 C_0(t_1)C_0(t_1+t_2)C_0(t_2+t_3)C_0(t_3) \tag{A2}$$

$$=\left(\frac{-iW}{\hbar}\right)^4\sum_k\sum_l\sum_p\sum_q h_k^2h_l^2h_p^2h_q^2$$

$$\times\int_0^\infty dt_1\int_0^\infty dt_2\int_0^\infty dt_3\exp[-i(\omega_k+\omega_l)t_1-i(\omega_l+\omega_p)t_2-i(\omega_p+\omega_q)t_3]. \tag{A3}$$

Because all ω_k are positive, each integral leads only to a principal value:

$$V_L|^{T=0}=\left(\frac{-iW}{\hbar}\right)^4\sum_k\sum_l\sum_p\sum_q h_k^2h_l^2h_p^2h_q^2\left(-iP\frac{1}{(\omega_k+\omega_l)}\right)\left(-iP\frac{1}{(\omega_l+\omega_p)}\right)\left(-iP\frac{1}{(\omega_p+\omega_q)}\right) \tag{A4}$$

and the value of the diagram is purely imaginary.

APPENDIX B

Here we show that for any system the ZPL shift and broadening are identical in the absorption and fluorescence spectrum. Since at $T=0$ K, the ZPL frequency in both absorption and fluorescence simply reflects the energy difference between the ground vibration states in the two electronic manifolds, it is clear that δ_0 will be identical in absorption and fluorescence. Thus we need only to show that the thermal broadening and shift are the same. Since the thermal broadening and shift are independent of a, in what follows we can safely neglect the linear electron–phonon coupling term.

The fluorescence line shape is given by[28]

$$I_{fl}(\omega)\propto\int_{-\infty}^{\infty}dte^{-i\omega t}e^{-|t|/2T_1}\langle e^{-iH_1t/\hbar}e^{iH_0t/\hbar}\rangle_1, \tag{B1}$$

where the subscript 1 indicates a thermal average over the *excited* state phonon Hamiltonian

$$\langle\cdots\rangle_1=\mathrm{Tr}_p[e^{-\beta H_1}\cdots]/\mathrm{Tr}_p[e^{-\beta H_1}]. \tag{B2}$$

Equation (B1) can also be written as

$$I_{fl}(\omega)\propto\int_{-\infty}^{\infty}dte^{-i(\omega-\omega_0)t}e^{-|t|/2T_1}\langle F_1(t)\rangle_1, \tag{B3}$$

where

$$F_1(t)=e^{iH_1t/\hbar}\exp-i(\Delta_1+H_1)t/\hbar \tag{B4}$$

and

$$\Delta_1=\frac{-W}{2}\phi^2. \tag{B5}$$

(We have neglected the linear term, as discussed above.) Since H_0 was taken to be harmonic and H_1-H_0 includes only quadratic terms, it follows that H_1 can be written as

$$H_1=\text{const}+\sum_k\hbar\omega_k'\,(b_k'^{+}b_k'+1/2), \tag{B6}$$

where ω_k' are the excited state normal mode frequencies and $b_k'^{+}$ and b_k' are the normal mode creation and annihilation operators. We can also express ϕ in terms of these normal mode operators.

$$\phi=\sum_k h_k'(b_k'^{+}+b_k'). \tag{B7}$$

Now we can perform the calculation of $\langle F_1(t)\rangle_1$ exactly as we did for $\langle F(t)\rangle$. Making the substitutions

$$W\rightarrow -W,\quad \omega_k\rightarrow\omega_k',\quad h_k\rightarrow h_k',$$

we can read off the results for the thermal loop cumulants from Eq. (84):

$$(K_T^{\text{loop}})^{fl}=-\int_0^{\infty}\frac{d\omega}{2\pi}\times\ln\left[1-\frac{iW2n(\omega)\Gamma_1(\omega)}{1+W\Omega_1(\omega)-iW\Gamma_1(\omega)}\right], \tag{B8}$$

where

$$\Gamma_1(\omega)=\frac{\pi}{\hbar}\sum_k h_k'^2\delta(\omega_k'-\omega), \tag{B9}$$

$$\Omega_1(\omega)=\frac{1}{\hbar}\sum_k h_k'^2\left\{P\frac{1}{\omega-\omega_k'}-\frac{1}{\omega+\omega_k'}\right\}. \tag{B10}$$

The thermal ZPL shift and broadening are obtained from [see Eq. (B3)]

$$\gamma^{fl}-i\delta_T^{fl}=-(K_T^{\text{loop}})^{fl}. \tag{B11}$$

It is not obvious that Eqs. (B8)–(B11) lead to results identical to those obtained in absorption from Eqs. (84) and (87). However, below we show that for $\omega>0$,

$$1+W\Omega_1(\omega)-iW\Gamma_1(\omega)=(1-W\Omega(\omega)+iW\Gamma(\omega))^{-1}, \tag{B12}$$

from which it follows that:

$$\frac{iW\Gamma(\omega)}{1-W\Omega(\omega)+iW\Gamma(\omega)}=\left(\frac{-iW\Gamma_1(\omega)}{1+W\Omega_1(\omega)-iW\Gamma_1(\omega)}\right)^*. \tag{B13}$$

With this, it is clear that

$$\gamma=\gamma^{fl}, \tag{B14}$$

$$\delta_T=\delta_T^{fl}. \tag{B15}$$

To derive Eq. (B12), we define the zero temperature Green's function

$$G(t)=\frac{-i}{\hbar}\langle 0|T\phi(t)\phi(0)|0\rangle, \tag{B16}$$

which is simply $-i/\hbar$ times $C(t)$ from Eq. (33), evaluated at $T=0$. (As in Eq. (33), $\phi(t)$ evolves in time with the ground state Hamiltonian H_0.) Taking the Fourier transform, from Eq. (46) we obtain for $\omega>0$

$$\hat{G}(\omega)=\Omega(\omega)-i\Gamma(\omega). \tag{B17}$$

Similarly we define another zero temperature Green's function

$$G_1(t)=\frac{-i}{\hbar}\langle 0'|T\phi_H(t)\phi_H(0)|0'\rangle, \tag{B18}$$

where $|0'\rangle$ is the ground state of the Hamiltonian

$$H=H_0+\frac{W}{2}\phi^2, \tag{B19}$$

and

$$\phi_H(t)=e^{iHt/\hbar}\phi\,e^{-iHt/\hbar}. \tag{B20}$$

Using Eqs. (B6) and (B7) and taking the Fourier transform, we obtain for $\omega > 0$

$$\hat{G}_1(\omega) = \Omega_1(\omega) - i\Gamma_1(\omega). \tag{B21}$$

Thus we need a relationship between $\hat{G}(\omega)$ and $\hat{G}_1(\omega)$. This is accomplished with the standard many body theory expansion[25]

$$G_1(t) = \lim_{\epsilon \to 0} \frac{-i/\hbar}{\langle 0|S|0\rangle} \sum_{n=0}^{\infty} \left(\frac{-iW}{2\hbar}\right)^n \frac{1}{n!} \times \int_{-\infty}^{\infty} dt_1 \cdots \int_{-\infty}^{\infty} dt_n \exp[-\epsilon(|t_1| + \cdots |t_n|)] \times \langle 0|T\phi(t_1)^2 \cdots \phi(t_n)^2 \phi(t)\phi(0)|0\rangle, \tag{B22}$$

where

$$\langle 0|S|0\rangle = \sum_{n=0}^{\infty} \left(\frac{-iW}{2\hbar}\right)^n \frac{1}{n!} \int_{-\infty}^{\infty} dt_1 \cdots \int_{-\infty}^{\infty} dt_n \times \exp[-\epsilon(|t_1| + \cdots |t_n|)] \times \langle 0|T\phi(t_1)^2 \cdots \phi(t_n)^2|0\rangle. \tag{B23}$$

Using Wick's theorem to calculate the matrix elements of time ordered products and realizing that all disconnected terms are cancelled by $\langle 0|S|0\rangle$,[25] we obtain

$$G_1(t) = G(t) + W \int_{-\infty}^{\infty} dt_1 G(t - t_1) G(t_1) + W^2 \int_{-\infty}^{\infty} dt_1 \int_{-\infty}^{\infty} dt_2 G(t - t_1) \times G(t_1 - t_2) G(t_2) + \cdots. \tag{B24}$$

Performing the Fourier transform and summing the series gives

$$\hat{G}_1(\omega) = \frac{\hat{G}(\omega)}{1 - W\hat{G}(\omega)}, \tag{B25}$$

from which immediately follows Eq. (B12).

[1] W. H. Hesselink and D. A. Wiersma, in *Spectroscopy and Excitation Dynamics of Condensed Molecular Systems*, edited by V. M. Agranovich and R. M. Hochstrasser (North-Holland, Amsterdam, 1983).

[2] M. J. Burns, W. K. Liu, and A. H. Zewail, in *Spectroscopy and Excitation Dynamics of Condensed Molecular Systems*, edited by V. M. Agranovich and R. M. Hochstrasser (North-Holland, Amsterdam, 1983).

[3] M. D. Fayer, in *Spectroscopy and Excitation Dynamics of Condensed Molecular Systems*, edited by V. M. Agranovich and R. M. Hochstrasser (North-Holland, Amsterdam, 1983).

[4] D. A. Wiersma, Adv. Chem. Phys. **47**, 421 (1981).

[5] A. A. Maradudin, Solid State Phys. **18**, 273 (1966).

[6] I. S. Osad'ko, in *Spectroscopy and Excitation Dynamics of Condensed Molecular Systems*, edited by V. M. Agranovich and R. M. Hochstrasser (North-Holland, Amsterdam, 1983).

[7] I. S. Osad'ko, Usp. Fiz. Nauk **128**, 31 (1979) [Sov. Phys. Usp. **22**, 311 (1979)].

[8] T. Holstein, S. K. Lyo, and R. Orbach, in *Laser Spectroscopy of Solids*, edited by W. M. Yen and P. M. Selzer (Springer, Berlin, 1981).

[9] R. Silbey, in *Spectroscopy and Excitation Dynamics of Condensed Molecular Systems*, edited by V. M. Agranovich and R. M. Hochstrasser (North-Holland, Amsterdam, 1983).

[10] G. J. Small, in *Spectroscopy and Excitation Dynamics of Condensed Molecular Systems*, edited by V. M. Agranovich and R. M. Hochstrasser (North-Holland, Amsterdam, 1983).

[11] P. M. Selzer, in *Laser Spectroscopy of Solids*, edited by W. M. Yen and P. M. Selzer (Springer, Berlin, 1981).

[12] D. E. McCumber and M. D. Sturge, J. Appl. Phys. **34**, 1682 (1963).

[13] M. A. Krivoglaz, Fiz. Tverd. Tela **6**, 1707 (1964) [Sov. Phys. Solid State **6**, 1340 (1964)]; Zh. Eksp. Teor. Fiz. **48**, 310 (1965) [Sov. Phys. JETP **21**, 204 (1965)].

[14] K. E. Jones and A. H. Zewail, in *Advances in Laser Chemistry*, edited by A. H. Zewail (Springer, New York, 1978).

[15] B. DiBartolo, *Optical Interactions in Solids* (Wiley, New York, 1968).

[16] F. P. Burke and G. J. Small, J. Chem. Phys. **61**, 4588 (1974); Chem. Phys. **5**, 198 (1974).

[17] I. I. Abram, Chem. Phys. **25**, 87 (1977).

[18] I. S. Osad'ko, Fiz. Tverd. Tela **13**, 1178 (1971); **14**, 2927 (1972); **17**, 3180 (1975) [Sov. Phys. Solid State **13**, 974 (1971); **14**, 2522 (1973); **17**, 2098 (1976)]; I. S. Osad'ko and S. A. Zhdanov, Fiz. Tverd. Tela **18**, 766 (1976) [Sov. Phys. Solid State **18**, 441 (1976)].

[19] G. J. Small, Chem. Phys. Lett. **57**, 501 (1978).

[20] J. L. Skinner, J. Chem. Phys. **77**, 3398 (1982).

[21] For an approach similar to Osad'ko's for a slightly different problem, see D. L. Tonks and B. G. Dick, Phys. Rev. B **19**, 1136 (1979); D. L. Tonks, *ibid.* **22**, 6420 (1980).

[22] D. Hsu and J. L. Skinner (to be submitted).

[23] R. G. Gordon, Adv. Magn. Reson. **3**, 1 (1968).

[24] R. Kubo, J. Phys. Soc. Jpn. **17**, 1100 (1962).

[25] A. L. Fetter and J. D. Walecka, *Quantum Theory of Many-Particle Systems* (McGraw-Hill, New York, 1971).

[26] R. Wertheimer and R. Silbey, J. Chem. Phys. **74**, 686 (1981).

[27] A calculation of the second cumulant with Abram's Hamiltonian shows that δ_T has a contribution of order W^2, in contrast to Abram's results.

[28] M. Lax, J. Chem. Phys. **20**, 1752 (1952).